

DEVELOPMENT OF LIGHTWEIGHT POTTERY USING ORGANIC AND INORGANIC ADDITIVES

Jae-Hwan Pee^{1,*}, Geun-Hee Kim¹, YooJin Kim², Jin-Ho Kim¹, Woo-Seok Kim¹, and Lada Punsukumtana³

Received: August 22, 2012; Revised: February 27, 2013; Accepted: March 8, 2013

Abstract

Organic poly-acrylonitrile hollow microspheres (OHM) and inorganic glass hollow microspheres (GHM) were used as pore-forming additives in a ceramic matrix. After sintering, the densities of the bodies were reduced. A change on the amount and the particle size of the pore-forming additives was observed. A pore membrane created with GHM inhibited the shrinkage in a sintered body. With the decrease in the body density, the water absorption rate increased by as much as 10% due to pore formation. The increase in pore volume of the sintered body results in the decrease in bending strength. A greater decrease in the bending strength and the fracture toughness of the OHM-added body were noted. The OHM decomposed below 500°C and did not influence the crystallization of the body. On the other hand, the GHM increased the amorphous glassy phases and cristobalite peak in the body after sintering. Finally, various pore microstructures were formed due to the size, the amount, and the type of the pore-forming additives.

Keywords: Lightweight, pottery, organic-inorganic pore foaming additives, porous, fracture toughness

Introduction

Tableware ceramics consist of raw materials with a high specific gravity above 2.6 g/cm³. These include kaolin, feldspar, and silica (Park and Lee, 1998). The needs for lightweight ceramic products are currently increasing (Rastoand David, 1989). A lightweight ceramic can be made by increasing the strength of the material and making it thinner. However, difficulties in the process,

such as the casting stage, hinder the manufacture of the thinner product (Crofts and Park, 1995).

In order to make lightweight ceramics, the most typical method used is creating pores in the ceramic body (Rastoand David, 1989; Crofts and Park, 1995; Kandori *et al.*, 2009; Cayre and Biggs, 2010). Two different methods can be used to create pores. The first method is to add pore-forming additives in the casting

¹ Traditional Ceramic Center, KICET, Icheon, Gyeonggi, 467-843, Korea. Tel.: 82-31-645-1426; Fax: 82-31-645-1487; E-mail: pee@kicet.re.kr

² Engineering Ceramic Center, KICET, Icheon, Gyeonggi, 467-843, Korea.

³ Department of Science Service, Bangkok, 10400, Thailand.

* Corresponding author

stage. Another method is to create pores during the sintering process (Jun *et al.*, 2006). Pore-forming additives added during the casting stage are either organic materials such as an organic hollow microsphere, poly methyl meth acrylate, etc. or inorganic materials such as a fly ash hollow microsphere, glass hollow microsphere, etc (Choi *et al.*, 2011; Kim *et al.*, 2011 a, b). The organic pore-forming additives will burn below 500°C, therefore both hollow and non-hollow spheres can be used. On the contrary, the inorganic pore-forming additives which do not combust after the sintering process will leave the residuals to remain in the sintered body. The inorganic pore-forming hollow sphere is usable (Gain and Lee, 2006). Some inorganic materials which are decomposed and then create pores during the sintering process at high temperature can also be used as inorganic pore-forming additives, for example carbon, hydroxyapatite (HAp), ceria (CeO₂), and pottery stone (KAl₂(AlSi₃O₁₀)(F,OH)₂) with fluorine (Gain and Lee, 2006) However, pore formations during the sintering process have difficulty in controlling a uniform pore size. Swelling may also be caused due to gasification of pore-forming additives and deformation of the ceramic body (Freiman, 1988; Takamitsu, 1990; Jeannine and Curtis, 1992; Furuta *et al.*, 1993). In contrast, pore-forming additives used during the casting stage can distribute pores evenly in the green body. Also both the sizing of the pores and the crystalline phase caused by the pore-forming additives are controllable.

In this study, both organic and inorganic pore-forming additives will be used to develop lightweight pottery. The effect of different types of pore-forming additives on the physical

properties and the sintering behavior will be evaluated.

Materials and Methods

The GoryeoDoto readymade body, 1S, widely used in Korea was used as the starting raw material. The slurry was prepared with 33 wt% of water. Table 1 shows the chemical compositions of the body clay and inorganic pore-forming additives. The particle size analysis of the body clay was measured using the laser diffraction method, and the mean particle size was 6.8 μm. Figure 1 shows the microstructure and the particle size distribution of the body clay. Poly-acrylonitrile hollow microspheres (OHM-A, B), and glass hollow microspheres (GHM-A, B) were used for the pore-forming additives. The GHM showed the glassy composition of SiO₂, Na₂O, CaO, and B₂O₃.

The microstructure of the pore-forming additives was observed by using a scanning electron microscope (SEM) (JSM-6390, JEOL Ltd., Tokyo, Japan). The particle size distribution of the pore-forming additives was measured by using a particle size analyzer (Dry Type, Beckman Coulter LS13320, Beckman Coulter Inc., Brea, CA, USA). All pore-forming additives showed a uniform sphere morphology and their mean particle sizes were in the range of 30~100 μm. Figure 2 shows the morphology of the pore-forming additives and Figure 3 shows the particle size distribution analysis of the additives. The additives' densities were measured by using a helium pycnometer (AccuPyc II-1340, Micromeritics Instrument Corp., Norcross, GA, USA) and the results show OHM-A to be 0.03 g/cm³, OHM-B to be

Table 1. Chemical compositions of raw materials and pore-forming additives (wt%)

Contents	SiO ₂	Al ₂ O ₃	Fe ₂ O ₃	CaO	MgO	K ₂ O	Na ₂ O	TiO ₂	P ₂ O ₅	B ₂ O ₃	Ig. loss
Body clay	71.60	18.90	0.36	0.31	0.19	1.75	1.16	0.03	0.03	-	5.28
GHM	72.00	0.08	0.07	12.40	0.23	0.01	6.34	0.01	0.70	7.73	-

0.025 g/cm³, GHM-A to be 0.350 g/cm³, and GHM-B to be 0.130 g/cm³. Table 2 shows the densities and mean particle sizes of the pore-forming additives.

In the S1 slurry with 33 wt% water, 0.0~0.8 wt% of OHM or 0.0~2.5 wt% of GHM was added. The slurry and the pore-forming additives were mixed for 10 min by using an ultrasonic disperser. The mixture was then cast in a plaster mold, dried for 40 min, and then taken out of the mold. The green body was dried at room temperature for 24 h before sintering at a temperature of 1250°C, with a 2°C/min heating rate and 30 min soaking time. The linear shrinkage of the sintered product was measured by

marking a linear line of 10 cm in the sample's long axis before and after the sintering process. The water absorption and density were measured by using the Archimedes method using a sample size of 12×17×3.5 mm. The microstructures of the sintered samples were observed by using an SEM. The 3 point bending strength test method at the cross head speed of 0.5 mm/min was used. Fracture toughness was measured by the single-edge V-notched beam method which was suitable for both dense and porous ceramics. The sample size of 40×4×3 mm was used for the bending strength test and fracture toughness test.

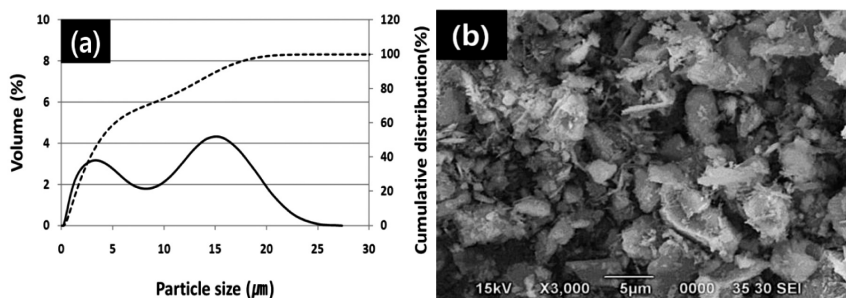


Figure 1. Particle size distribution (a) and microstructure (b) of the body clay

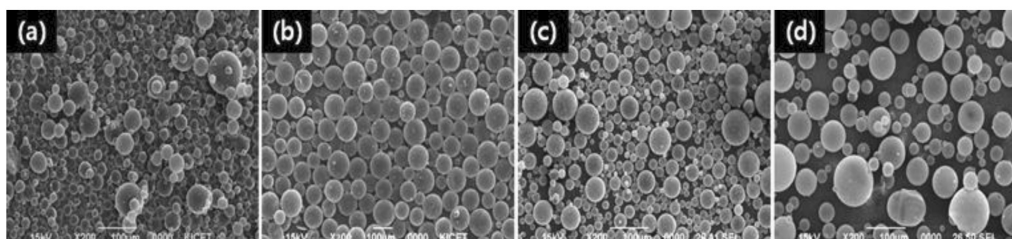


Figure 2. Microstructures of pore-forming additives (a) OHM-A (b) OHM-B (c) GHM-A and (d) GHM-B

Table 2. Densities and mean particle sizes of pore-forming additives

	OHM		GHM	
	A	B	A	B
Density (g/cm ³)	0.030	0.025	0.350	0.130
Particle mean size (µm)	30	100	30	50

Results and Discussion

The bulk density of the sintered bodies is shown in Figure 4. Samples without the pore-forming additive showed a bulk density of 2.42 g/cm³. Figure 4(a) shows the bulk density of the sample with the organic pore-forming additive. The bulk density of the OHM-B greatly decreased with an increase in the size and the amount of the pore-forming additives. The mean 100 μm size OHM-B

with 0.8 wt% additions showed the lowest bulk density of 1.2 g/cm³. Figure 4(b) shows the bulk density of the sample with the inorganic pore-forming additive. A steady decrease in bulk density with an increase in the amount of the inorganic pore-forming additive was found. A sample with 2.5 wt% of GHM-B showed the lowest bulk density of 1.5 g/cm³. The density and the residual glassy substance of the GHM in the matrix after the sintering process causes 20% higher bulk density than

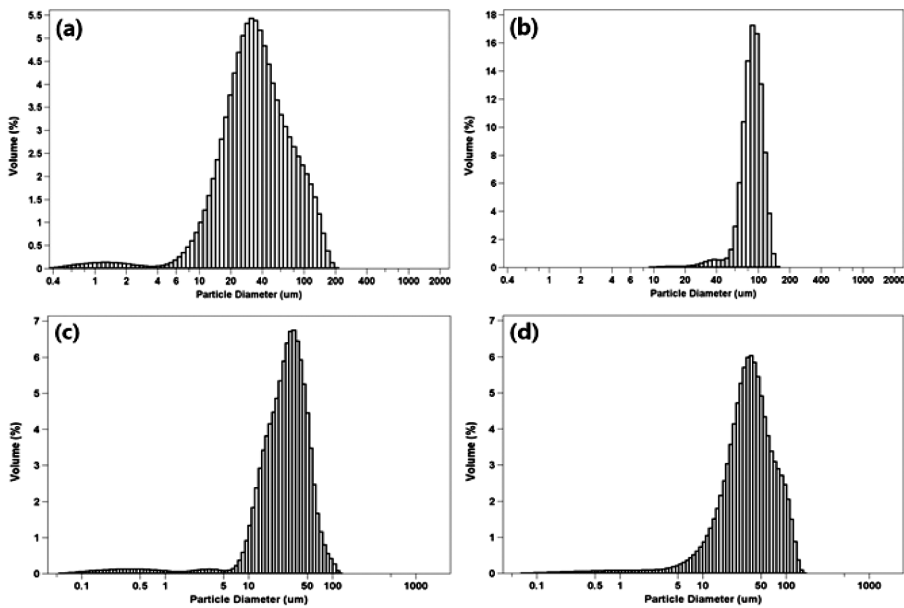


Figure 3. Particle size analysis of pore-forming additives (a) OHM-A, (b) OHM-B, (c) GHM-A and (d) GHM-B

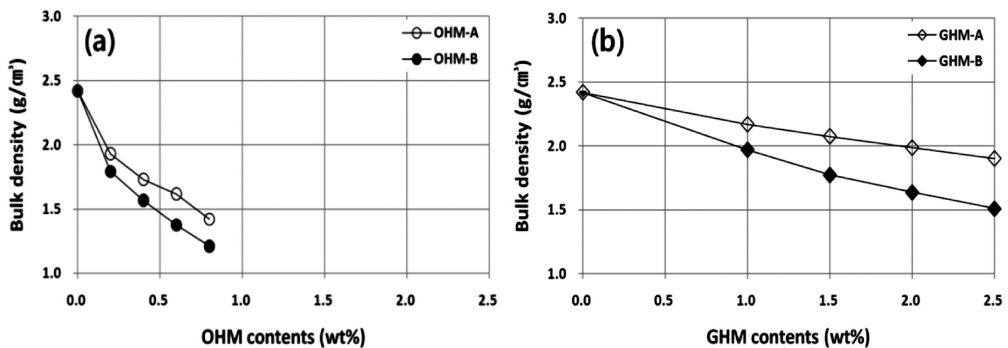


Figure 4. Bulk density of the sintered body with different pore-forming additives (a) organic and (b) inorganic

the bulk density of the OHM-added samples. In general, it was verified that the change in the bulk density resulted from the contents, additive sizes and density of the pore-forming additives.

The linear shrinkage of the sintered body fired at 1250°C is shown in Figure 5. The linear shrinkage rate of the sample without the pore-forming additives is 12.15%. An increase in the linear shrinkage with a decrease in the density of the sintered body with OHM can be seen in Figure 5(a). Organic pore-forming additives are combusted and formed open type pores below a temperature of 500°C. At a temperature over 1100°C, the densification process progressed. On heating, the matrix and the pores shrink which increases the shrinkage rate. Figure 5(b) shows the shrinkage of the sintered body with the

addition of the inorganic pore-forming additive. However, Figure 5(b), in contrast to Figure 5(a), showed an increase in the density of the sintered body with an increase in shrinkage. The sample with the GHM showed a slight change in the shrinkage range lower than 1%. The GHM creates an amorphous phase during the densification process which promotes the densification behavior of the ceramic material. The GHM, by its nature, does not combust after sintering and remains in the matrix and forms the closed pore membrane with a glass shell. This glass shell and membrane inhibit the shrinkage.

The sintered bodies with the pore-forming additives can absorb water as can be seen in Figure 6. The water absorption rate of the sintered body without the pore-forming additives is 0.22%. Both the OHM and

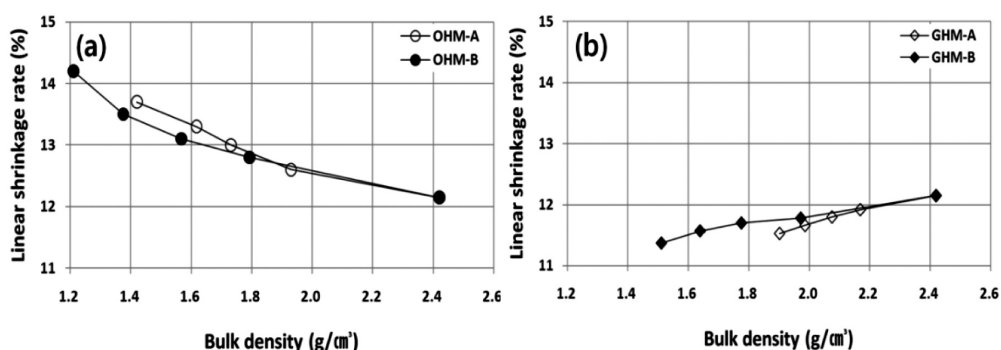


Figure 5. Linear shrinkage rate by adding pore-forming additives (a) organic and (b) inorganic

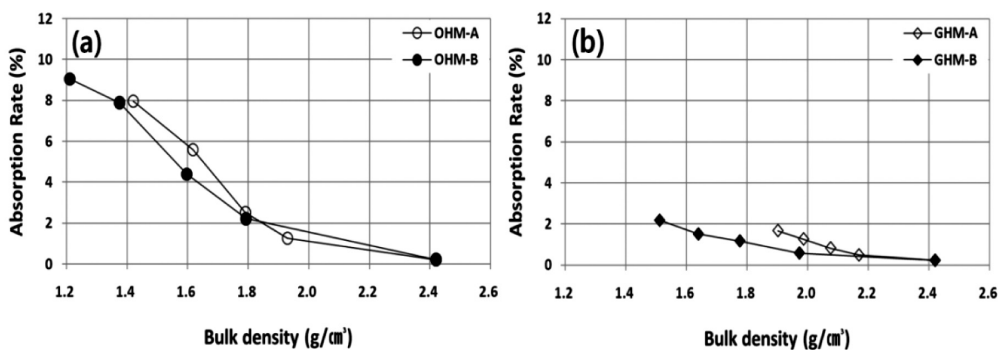


Figure 6. Water absorption rate by adding pore-forming additives (a) organic and (b) inorganic

GHM-added samples showed a higher water absorption rate when the sample density decreases. Figure 6(a) shows the water absorption rate of the samples with the OHM addition. The OHM leads to an increase of the open pore formation process. These open pores created a connecting structure which results in a high water absorption rate. Figure 6(b) shows the absorption rate of the sample with the GHM addition. The GHM formed the closed pore membrane in the matrix after sintering. Therefore, the body with the GHM addition showed a lower absorption rate than the organic pore-forming additive did. The results showed that a decrease in the density of the sintered body with both pore-forming additives resulted in an increase in the water absorption properties. The organic pore-forming materials form open pores which result in a higher water absorption rate than the inorganic pore-forming materials which form closed pores. At the same volume matrix, open pores occupy more matrix proportions and thus decrease the density and increase the absorption rate. Also, open pores are internally connected through the surface of the sintered body, therefore increasing the water absorption value.

Figure 7 shows the crystal phase analysis of the different pore-forming additives added to the sintered sample. In the

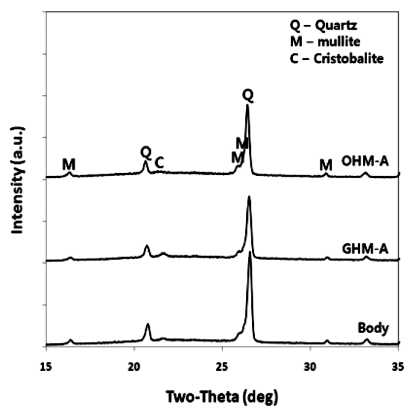


Figure 7. Crystal phase analysis of the sintered body

analysis of the sintered body without the pore-forming additives, quartz (SiO_2), mullite ($\text{Al}_4\text{Si}_2\text{O}_{13}$), and cristobalite (SiO_2) are found as the major crystal phases. The OHM had little influence on the crystal phase of the sintered body. This is because the OHM was burnt below 500°C , thus not influencing the crystallization process. On the other hand, the crystal phase change was found in the sintered body with the GHM addition. The amorphous phase was more than in the other sintered bodies. The cristobalite phase also increased due to an increase of the SiO_2 amount, therefore decreasing the peak intensity of the quartz phase. As a result, it is confirmed that the OHM does not have an influence on the crystallization process of the body whereas the GHM can affect the crystallization process of the body.

Figure 8 shows the relationship between the bending strength and density of the samples fired at 1250°C . The 3 point bending test of the sintered body without the pore-forming additive showed a bending strength of 110 MPa at the density of 2.42 g/cm^3 . Figure 8(a) shows the bending strength of the sintered OHM-added body. With the OHM-B-added sample having a mean particle size of $100 \mu\text{m}$, the bending strength decreased drastically. OHM-A-added sample having a mean particle size of $30 \mu\text{m}$ showed a 5% higher bending strength than the OHM-B sample. Also it was verified that an increase of the amount of pore-forming additives showed a decrease in the bending strength. Figure 8(b) shows the bending strength results of the GHM-added sintered body. As shown in Figure 8(b), with an increase of the pore-forming additive volume, the bending strength decreased. As the density decreases, the strength also decreased. This is because the pore volume in the sintered body increases.

The relationship of the fracture toughness and the density of the different pore-forming additives added to the sintered body is shown in Figure 9. The sintered body without the pore-forming additive showed the highest fracture toughness of $1.22 \text{ MPam}^{1/2}$. It was verified that at the same given density,

the fracture toughness showed different results in accordance with the different type of the pore-forming additives and various particle sizes. For the OHM-added sintered body, with the decrease in the density the fracture toughness decreased to 0.87~0.46 MPam^{1/2}. The GHM-added sintered body showed a similar tendency with the OHM-added body with the fracture toughness ranging from 0.91 MPam^{1/2} to 0.44 MPam^{1/2}. A different pore volume in the sintered body results in a different speed of crack propagation. It is considered that the fracture toughness changes in accordance with the after-sintering characteristics of the organic and inorganic materials. GHM-B has about a 50 μm smaller size than the OHM-B, and creates a glass shell around the pore after the

sintering process. Therefore the fracture toughness is higher. The results show that pore formation leads to a greater decrease in bending strength compared to the decreased proportion of the fracture toughness. Also, at a similar density, the result of the fracture toughness and bending strength showed a high correlation.

The microstructure of the sintered body is shown in Figure 10. Figure 10(a) is the microstructure of the sample without the pore-forming additives and it can be seen that there are no pores and it is highly vitrified. Figure 10(b) shows the fracture surface of the OHM-A-added sample and it was verified that many pores are formed which have a 5~10 μm lower particle size than the mean particle size of the OHM before the sintering process.

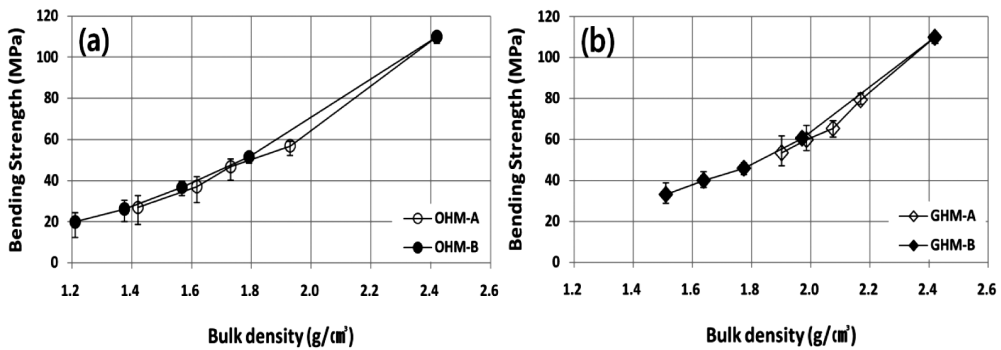


Figure 8. Bending strength by adding pore-forming additives (a) organic and (b) inorganic

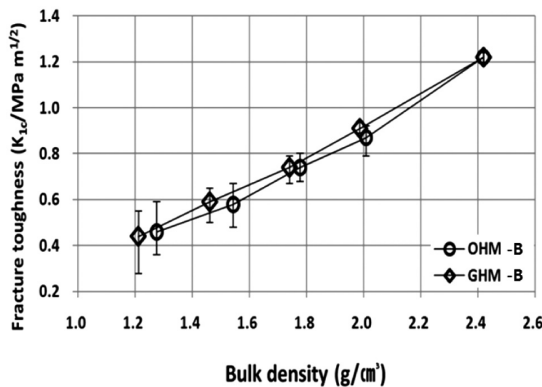


Figure 9. Fracture toughness by bulk density and type of pore-forming additives.

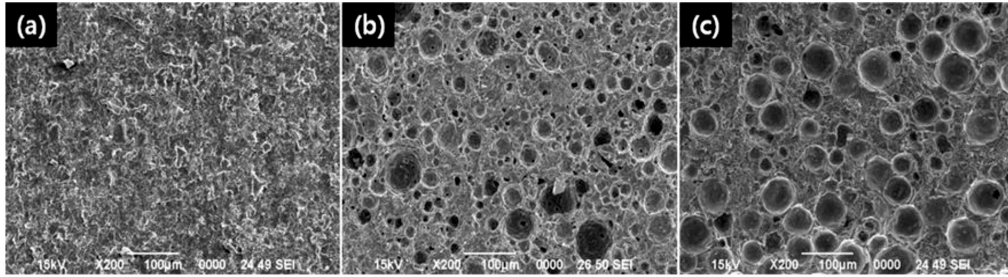


Figure 10. Microstructures of lightweight sintered body (a) Additive-free, (b) OHM-A and (c) GHM-A

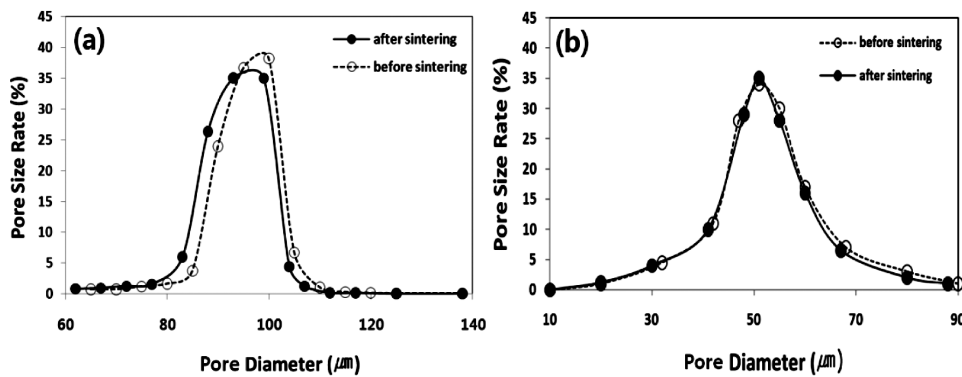


Figure 11. Pore distribution of the sintered body (a) organic and (b) inorganic

Figure 11 shows the pore size distribution of the organic and inorganic additives and pores before and after the sintering process. It is considered that such a reduction of pore size occurs because the densification process of the matrix accompanied the pore shrinkage. However, in the GHM-A-added sample shown in Figure 10(c), the mean particle size of the pore-forming additives and the size of the pores created after the sintering process are shown to be similar. It is because the inorganic additives remained as a glass shell in the matrix and inhibited the pore shrinkage after sintering.

Conclusions

Organic (OHM) and inorganic (GHM) pore-forming additives were added to make a lightweight ceramic. The organic and inorganic pore-forming additives formed pores in the ceramic matrix after the sintering

process and reduced the density. The OHM-added sintered body had a low specific gravity reduced by around 40% density. It was observed that the density change occurs due to the specific gravity, the particle size, and amount of the pore-forming additives. Also OHM burns below 500°C forming pores after the sintering process. These pores shrank with the matrix therefore increasing the shrinkage rate. The GHM-added sintered body creates a glass shell and pore membrane after the sintering process which inhibits the shrinkage. With the decrease in density, the absorption rate increases by as much as 10% due to the pore formation. Also with the decrease in density, the volume of the pores in the sintered body increases, therefore decreasing the bending strength. A greater decrease in the bending strength was shown compared to the decreased proportion of the fracture toughness value. Also the fracture toughness and bending strength showed a high correlation.

It was shown that the OHM, which burns below 500°C, does not influence the crystallization. On the other hand, the GHM increased the amorphous phases and cristobalite due to the residual glassy substance after the sintering process. Finally, observations of the microstructures showed that variable pores are formed due to the size and the amount of the pore-forming additives.

Acknowledgements

This work was supported by the “Policy R&D Program” funded by the Korea Institute of Ceramic Engineering and Technology, Korea.

References

- Cayre, O.J. and Biggs, S. (2010). The role of particle technology in developing sustainable construction materials. *Adv. Powder Technol.*, 21:19-22.
- Chantikul, P., Anstis, G.R., Lawn, B.R., and Marshall, D.B. (1981). A critical evaluation of indentation techniques for measuring fracture toughness: II, strength method. *J. Am. Ceram. Soc.*, 64:539-543.
- Choi, H.S., Pee, J.H., Kim, G.H., Kim, Y.J., Cho, W.S., and Kim, K.J. (2011). Effect of PAHM (poly-acrylonitrile hollow microsphere) addition on the lightweight and firing behavior of whiteware. *Mater. Sci. Eng.*, 18:222-029.
- Crotts, G. and Park, T.G. (1995). Preparation of porous and nonporous biodegradable polymeric hollow microspheres. *J. Control. Release*, 35:91-105.
- Freiman, S.W. (1988). Brittle fracture behavior of ceramics. *J. Am. Ceram. Soc.*, 67:392-402.
- Furuta, S., Nakao, H., and Katsuki, H. (1993). Preparation of porous ceramics from industrial waste silica mineral. *J. Mater. Sci. Lett.*, 12:286-287.
- Gain, A.K. and Lee, B.T. (2006). Microstructure control of continuously porous t-ZrO₂ bodies fabricated by multi-pass extrusion process. *Mater. Sci. Eng.*, 419:269-275.
- Jeannine, S.W. and Curtis, E.S. (1992). Processing of porous ceramics. *J. Am. Ceram. Soc.*, 71:1674-1682.
- Jun, I.K., Koh, Y.H., Song, J.H., Lee, S.H., and Kim, H.E. (2006). Improved compressive strength of reticulated porous zirconia using carbon coated polymeric sponge as novel template. *Mater. Lett.*, 60:2507-2510.
- Kandori, K., Takeguchi, K., Fukusumi, M., and Morisada, Y. (2009). Applications of microporous glass membranes. *Polyhedron*, 28:3036-3042.
- Kim, G.H., Choi, H.S., Pee, J.H., Cho, W.S., and Kim, K.J. (2011). Lightweight porcelain using GHM (glass hollow microsphere). *J. Kor. Ceram. Soc.*, 48:74-79.
- Kim, G.H., Pee, J.H., Kim, Y.J., Cho, W.S., and Kim, K.J. (2011). Lightweight characteristics and sintering behavior of porcelain by addition FAHM (fly-ash hollow microsphere). *J. Kor. Ceram. Soc.*, 48:228-235.
- Park, J.K. and Lee, J.S. (1998). Preparation of porous inorganic materials by foaming slurry. *J. Kor. Ceram. Soc.*, 35:1280-1285.
- Rasto, B. and David, J.G. (1989). Fracture behavior of open-cell ceramics. *J. Am. Ceram. Soc.*, 72:1145-1152.
- Takamitsu, F. (1990). Processing and properties of cellular silica synthesized by foaming sol-gels. *J. Am. Ceram. Soc.*, 73:85-90.
- Thorby, P.N. and Ferguson, W.G. (1976). The fracture toughness of HY 60. *Mater. Sci. Eng.*, 22:177-184.
- Wang, S.R., Geng, H.R., Hui, L.H., and Wang, Y.Z. (2006). Reticulated porous multiphase ceramics with improved compressive strength and fracture toughness. *J. Mater. Eng. Perform.*, 16:113-118.

